TB28

19th International Symposium of Ballistics, 7–11 May 2001, Interlaken, Switzerland

THE INFLUENCE OF PENETRATOR GEOMETRY AND IMPACT VELOCITY ON THE FORMATION OF CRATER VOLUME IN SEMI-INFINITE TARGETS

N.J. Lynch[1], R. Subramanian[2], S. Brown[1], J. Alston[2]

[1] DERA Fort Halstead, Sevenoaks, Kent, UK
[2] The Institute for Advanced Technology, Austin, Texas, USA

Crater volumes in semi-infinite steel targets have been measured for a range of penetrator shapes and aspect ratios. The impact velocities range from 1.8 to 2.9 km/s. The penetrators were of constant mass (60 grams) made from tungsten alloy, and were fired into the same parent RHA plate. The trends in impact energy/crater volume (E/V) show a reduction with increasing velocity, but there is still an L/D effect at 3 km/s. E/V values for an L/D 4.5 unitary rod and two novel penetrator designs (segmented and telescopic) approximately followed their effective aspect ratios at 1.8 km/s. An L/D 20 penetrator was found to have a low E/V efficiency.

INTRODUCTION

This paper presents an analysis of crater volumes in Rolled Homogeneous Armour (RHA) steel targets, produced by various shapes of tungsten alloy penetrators. A number of surveys of hole volume relationships have been produced previously [1,2]. Hohler and Stilp found crater volumes at low ordnance velocity to be dependent on the length to diameter (L/D) ratio of the penetrator, but this dependency disappeared at higher velocities. Murphy examined impact energy normalised by crater volume (E/V) and observed a minima in E/V for RHA at 5 km/s. The E/V ratio has been applied more frequently to spheres than the more conventional long rod penetrators for which penetration depth is the key concern. Nevertheless, E/V supports the efforts of analytical modelers, and studies into the lethality of novel penetrators.

EXPERIMENTAL PROCEDURE

Projectiles and targets

Four penetrator designs, all of nominal mass 60 grams, were fired against semi-infinite armor steel at velocities between 1.8 and 2.9 km/s. The designs are shown in Figure 1 and consisted of two unitary projectiles of length to diameter ratio (L/D) 4.5 and 20:1, a 3

segment segmented rod and a telescopic design with a 6 mm diameter rod. The penetrator material was Plansee D176, a 92%W-Ni-Fe alloy.

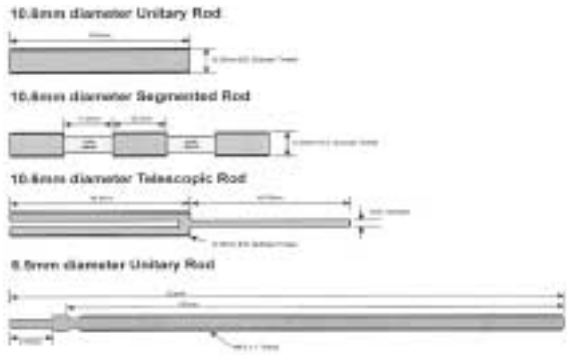

Figure 1. Penetrator designs.

The target material was Rolled Homogeneous Armour (RHA) with a Brinell hardness of 255 to 262. All the target material was taken from the same 150 mm thick parent plate, cut into 180 mm square blocks. The testing methodology and depth of penetration measurements have been reported previously [3, 4]. For completeness, the penetration depth vs. velocity is shown in Figure 2.

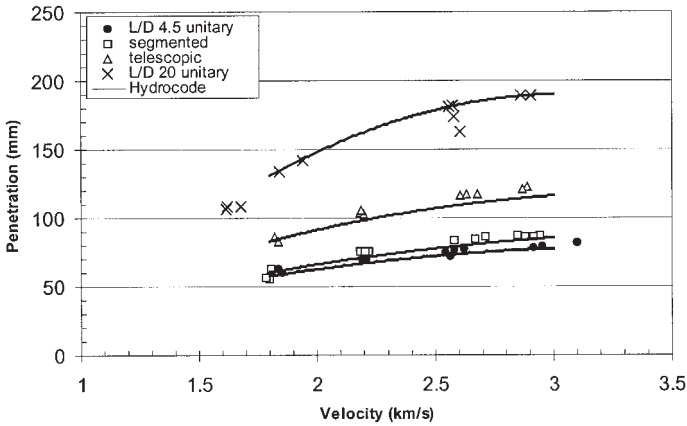

Figure 2. Penetration depth into RHA vs. velocity.

This paper addresses the crater volume measurements and the corresponding values for impact energy normalized by crater volume (E/V) from these tests.

EXPERIMENTAL RESULTS

Measured crater volumes and the resultant values for E/V are listed in Table 1, together with details of the impact conditions. The crater volumes were measured to the original impact surface of the target and hence do not include the volume contained by the "crater lip" pushed up during the initial stages of penetration. Although this approach neglects a portion of the apparent crater volume, it is consistent with the manner in which penetration depths are typically measured. Similarly, because the intent was to measure the volume of target material displaced, the volumes listed include the estimated volume

of any residual penetrator material at the bottom of the crater. The details of the measurement procedures are given in the following paragraphs.

For the lower velocity tests (1.8 and 2.2 km/s), two orthogonal radiographs of the crater were taken with through-target x-rays. The crater volume was then calculated from the digitized outline of the crater profile assuming axisymmetry about the local centreline. The average value of the two calculations is reported in this paper.

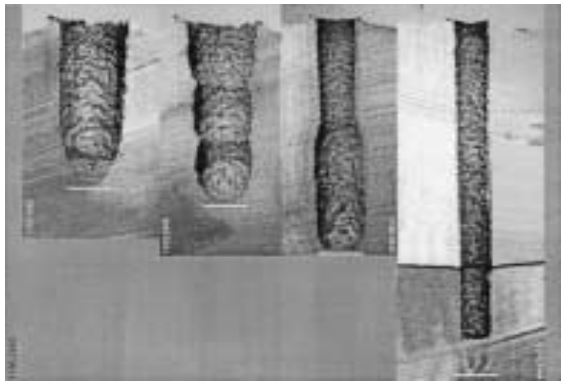

Figure 3. Crater shapes at 2.6 km/s. From left: Unitary, segmented, telescopic, 6.5 mm unitary.

Figure 3 shows typical crater shapes produced by the 4 designs at 2.6 km/s.

For the higher velocity tests (2.6 and 2.9 km/s) crater volumes were measured by direct liquid fill. The two halves of the previously sectioned target were clamped together and the crater was filled to the level of the original impact surface. A cork gasket placed between the two sections scaled the interface and corrected for material lost during sectioning (~1.5 mm). The estimated volume of any residual penetrator material at the bottom of the crater was added to the fill volume to obtain the total crater volume. Total crater volume was checked against the volume computed from a digitized outline of the profile; in the few cases where the target halves could not be adequately clamped together this volume is reported.

COMPUTATIONAL RESULTS

Simulations of the experiments were carried out using the DERA GRIM2D Eulerian hydrocode. Cell sizes of 1 mm square were used for the short unitary and segmented designs, reducing to 0.75 mm square for the telescopic and 6.5 mm diameter unitary rods. Relatively simple elastic-plastic material constitutive models were used for the RHA and tungsten. The penetration depth from the simulation was in very good agreement with the lowest yaw experiments, as shown in Figure 2. The craters from the simulations were then digitised in a similar manner to the experiments. The crater profile followed the interface between the target material and the residual penetrator material, all of which remained in the crater. The results are discussed in the following section.

OBSERVATIONS

The ratio of impact energy to crater volume (E/V) obtained in the experiments and the simulations is plotted in Figure 4. The experimental scatter is more pronounced at the lower velocities (partly because the L/D 20 rod becomes more yaw sensitive at low velo-

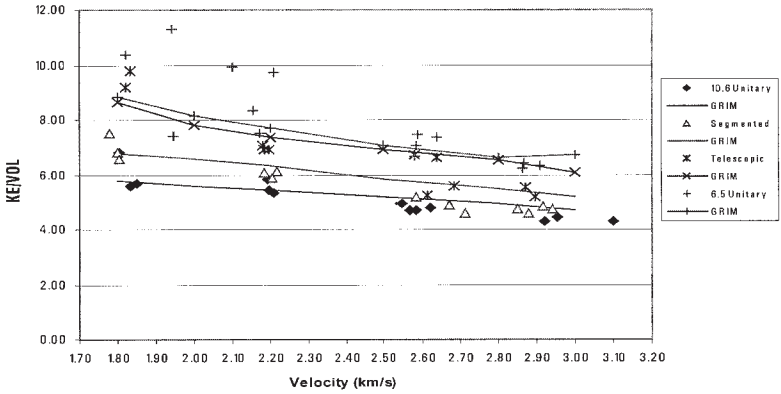

Figure 4. KE/VOL vs. velocity for the 4 designs.

cities, and absolute volume measurements are less), but two key trends may be observed in this plot: E/V decreases with impact velocity and increases with the aspect ratio of the penetrator. These observations existed in both the experiments and the simulations, although the relative magnitudes differ.

A general decrease in E/V with impact velocity exists for each of the four penetrator types. It is not possible to determine whether this decrease is asymptotic to a common value or a minimum in E/V versus velocity curve. In the simulations the decrease is approximately 25% over the range of velocities tested regardless of the type of penetrator. The experimental data show similar trends. For the 10.6 mm unitary and segmented penetrators, the data closely followed the simulations, although the offset between the two sets of data was slightly less at higher velocity than was observed in the simulations. For the telescopic penetrator, the data decreased more rapidly than observed in the simulations, being somewhat higher than predicted at the lower velocities and more closely matching the 10.6 mm designs at the higher velocities. The simulations show the E/V trends for the 6.5 mm unitary rod to be similar to those of the telescopic penetrator, although the lower velocity data for this design were significantly higher, and more widely scattered, than in the simulations.

The decrease in E/V follows the decrease in the fraction of impact energy spent in deformation of the penetrator [5]. This supports the suggestion that E/V is constant for a given penetrator/target material pair [6–8] provided that E is considered as only the energy spent in formation of the crater. Otherwise E/V is not independent of L/D and velocity at impacts up to 3 km/s.

The second observation, that E/V increases with increasing aspect ratio of the penetrator, is less clear. For these novel penetrators we considered an aspect ratio based on the mass effective diameter (L/Deff). In order of increasing aspect ratio (i.e., length) these values are: 4.6, 8.5, 12, and 23. The trend of E/V increasing with aspect ratio is most evident at lower velocities, at which E/V for the 6.5-mm unitary rod (L/D~20) is approximately twice that ofthe 10.6 mm unitary rod (L/D~5). The data for the other two designs tend to fall between these two bounds. The simulations follow these trends, but for the two rod designs the E/V difference is less: about 60%. Also, the simulations show nearly identical values for the 6.5 mm unitary rod and the telescopic penetrator despite a significant diffe-

rence in L/Deff. Although higher aspect ratio penetrators may be less efficient in terms of the formation of crater volume, it should be noted that the opposite is true for efficiency in terms of penetration depth.

We compared these data with those available in the literature [1,2,6,9]. For long rods (L/D~20) these references list values for E/V decreasing from approximately 7 KJ/cc at 1.8 km/s to 5 KJ/cc at 3.0 km/s. The data reported herein for the 6.5 mm unitary rod (L/D 23) are somewhat higher than this, particularly at the lower velocities. The data for the 10.6 mm unitary and segmented penetrators more closely follow reported values, falling between the data for L/D 1 and 10 rods in [1]. Overall, the trends match the observations of Murphy [2] and also Ref [6].

The telescopic design is an interesting hybrid. The rod section has an L/D of nearly 7 and contains 32% of the penetrator mass. For the higher velocity tests, the fraction of crater volume that appears to be created by this portion of the penetrator (i.e., prior to opening up of the crater diameter) is also approximately 30%, suggesting that the L/D 7 rod portion and the following tube portion have approximately equal values of E/V (~5.5 KJ/cc). Other data gives 5.48 KJ/cc at 2.5 km/s for an L/D 7 rod [10].

This observation was investigated further. Comparison of average crater diameter in the two sections of the crater showed that the tubular portion displaced an equal amount of material laterally. This is shown in Figure 5, in which the average normalized crater diameter (d) for the two portions of the telescopic crater is plotted for the higher velocity tests (a mass effective diameter of 8.0 mm was used for the tube section).

Also included in this plot are the data from the 6.5 mm and 10.6 mm unitary rods, and a d/D fit from other experimental data [11]. Simulations of equivalent mass (60 g) tubular penetrators yielded equivalent values for E/V and nearly identical crater diameters. These results suggest that at these velocities tubes are as efficient as rods in terms of volume displaced and penetration depth.

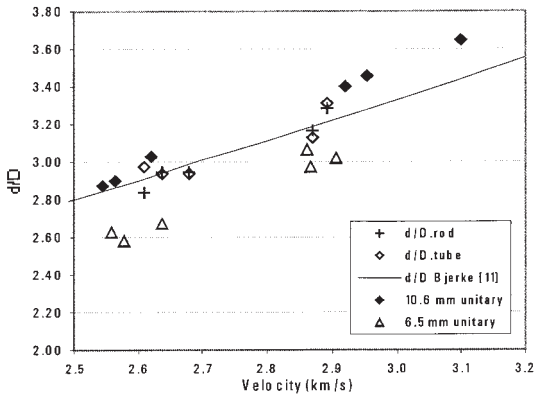

Figure 5. Crater dia./mass effective rod dia. vs. velocity.

CONCLUSIONS

Crater volume data were obtained with four penetrator geometries impacting semi-infinite armor steel targets. Equivalent mass tungsten penetrators and consistent penetrator and target material properties allowed a direct comparison of the efficiency of crater formation, quantified as the ratio of impact energy to resultant crater volume. The experiments were conducted at impact velocities ranging from 1.8 to 3.0 km/s and were supported by 2-D axisymmetric hydrocode simulations.

E/V values for an L/D 4.5 unitary rod and two novel penetrator designs (segmented and telescopic) were ranked by their effective aspect ratios at 1.8 km/s. An L/D 20 penetrator was found to have a low E/V efficiency for crater formation. Analysis of the telescopic design showed that tubolar penetrators arc as efficient as solid rods.

E/V ratios were still converging at the highest velocity examined (3 km/s). Hydrocode simulations followed the same trends as the experiments.

Table 1. Experimental Results

SHOT #	PENETRATOR TYPE	MASS (g)	VELOCITY (Km/sec)	TOTAL YAW (deg)	KE (KJ)	VOLUME (cc)	PLUG VOL. (cc)
57	10.6-mm Unitary	62.15	2.58	12.5	207.2	44.4	0.62
59		61.03	2.56	6.3	200.6	42.9	1.10
60*		62.46	2.62	3.8	214.5	44.9	
61		62.36	2.92	3.1	265.7	62.0	2.54
62		62.29	2.95	1.0	271.8	60.9	1.00
66		61.94	2.55	1.1	200.6	40.6	1.93
67*		62.11	3.10	0.8	298.4	69.6	
X362		62.05	1.81	1.1	101.1	14.9	
X363		61.93	1.83	1.0	104.0	18.6	
X364		62.1	1.85	1.5	106.3	18.7	
X371		62.08	2.19	3.6	149.4	25.7	
X372		61.07	2.21	3.6	148.9	28.0	
X373		62.5	2.20	4.3	151.1	27.9	
58	Segmented	62.91	2.58	n/a	209.5	40.4	
68		62.84	2.71	1.4	231.3	50.2	
69		63.09	2.88	4.8	261.5	56.7	
72		62.96	2.85	3.3	255.9	53.8	
75		62.76	2.67	2.1	223.4	45.5	
81		62.42	2.94	1.7	270.3	57.0	
82		62.93	2.92	0.7	267.5	55.5	
x368		60.75	1.80	n/a	98.4	14.4	
x369		60.98	1.78	n/a	96.7	12.9	
x370		61.5	1.81	n/a	100.2	15.3	
X377		61.4	2.18	n/a	146.3	24.1	
X378		62.05	2.22	n/a	152.8	25.0	
X379		61.84	2.20	n/a	150.2	25.5	
79*	6.5-mm Unitary	57.57	2.58	2.6	191.3	28.7	
80		58.1	2.59	5.1	194.3	26.0	
85		57.93	2.58	3.2	193.1	27.4	
89*		59.22	2.91	2.6	250.2	39.5	
90		59.36	2.86	2.8	243.1	39.1	1.38
93*		59.25	2.64	1.0	205.8	28.0	
95		58.18	2.87	0.4	238.9	37.3	2.47
X380		58.78	2.21	1.4	143.3	14.7	
X384		58.4	1.82	1.0	96.8	9.3	
X3090		59.15	1.95	1.1	112.1	15.1	
X3091		58.86	1.94	0.1	111.0	9.8	

Table1 (contd)

SHOT #	PENETRATOR TYPE	MASS (g)	VELOCITY (Km/sec)	TOTAL YAW (degrees)	KE (KJ)	VOLUME (cc)	PLUG VOL. (cc)
73	Telescopic	61.93	2.68	3.0	222.4	39.7	
74		62.34	2.61	1.2	212.2	40.4	2.88
76		62.28	2.58	6.1	206.6	30.7	
83		62.26	2.64	3.4	216.3	32.7	
84		62.03	2.89	2.2	259.6	50.2	2.10
86		62	2.87	1.1	255.2	46.3	
X366		61.98	1.83	2.2	104.2	10.6	
X367		62.4	1.82	3.0	103.5	11.3	
X374		62.15	2.18	1.6	147.7	21.0	
X375		62.11	2.20	2.1	150.2	21.7	
X376		61.97	2.19	1.0	148.1	21.5	

REFERENCES

1. V. Hohler and A. Stilp, “Influence of the Length-to-Diameter Ratio in the range from 1 to 32 on the Penetration Performance of Rod Projectiles,” 8th Intnl. Symp. Ballistics, Orlando, USA, 1984
2. M. J. Murphy, “Survey of the Influence of Velocity and Material Properties on the Projectile Energy/Target Hole Volume Relationship,” 10th Intnl. Symp. Ballistics, San Diego, USA, 1987
3. C. Brissenden, “Performance of Novel KE Penetrator Designs over the Velocity Range 1600 to 2000 m/s,” 13th Intnl. Symp. Ballistics, Stockholm, Sweden, 1992
4. N. Lynch et al, “Terminal Ballistic Performance of Novel KE Projectiles,” 15th Intnl. Symp Ballistics, Jerusalem, Israel, 1995
5. C. Anderson et al, “Long Rod Penetration, Target Resistance, and Hypervelocity Impact,» Intnl. J. Impact Eng. 14, 1993
6. D. R. Christman and J. W. Gehring, “Analysis of High-velocity Projectile Penetration Mechanisms,” J. Appl. Phys. 37 (4), 1966
7. T. Szendrei, “Link Between Axial Penetration and Radial Crater Expansion in Hypervelocity Impact,” 17th Intnl. Symp. Ballistics, Midrand, South Africa, 1998
8. T. Szendrei, “Analytical model for high-velocity impact cratering with material strengths:extensions and validation,” 15th Intnl. Symp. Ballistics, Jerusalem, Israel, 123–131, 1995
9. G. Silsby, “Penetration of Semi-infinite Steel Targets by Tungsten Long Rods at 1.3 to 4.5 km/s,” 8th Intnl. Symp. Ballistics, Orlando, USA, 1984
10. V. Hohler and A. Stilp, “Penetration performance of segmented rods at different spacings – comparison with homogeneous rods at 2.5–3.5 km/s”, 12th Intnl. Symp. Ballistics, San Antonio USA, 178–187, 1990
11. T. Bjerke, G. F. Silsby et al, “Yawed long-rod armour penetration penetration”, Int. Jnl. of Impact Engng. 12: 281–292, 1992.